

# Urban Heat Island Intensity Prediction in the Context of Heat Waves: An Evaluation of Model Performance <sup>†</sup>

Aner Martinez-Soto <sup>1,2,\*</sup> , Johannes Fürle <sup>2</sup> and Alexander Zipf <sup>2,3</sup>

<sup>1</sup> Department of Civil Engineering, Faculty of Engineering and Science, Universidad de La Frontera, Temuco 4780000, Chile

<sup>2</sup> GIScience, Institute of Geography, University of Heidelberg, 69120 Heidelberg, Germany; johannes.fuerle@uni-heidelberg.de (J.F.); zipf@uni-heidelberg.de (A.Z.)

<sup>3</sup> Heidelberg Institute for Geoinformation Technology gGmbH, 69118 Heidelberg, Germany

\* Correspondence: aner.martinez@ufrontera.cl; Tel.: +56-45-2596816

<sup>†</sup> Presented at the 9th International Conference on Time Series and Forecasting, Gran Canaria, Spain, 12–14 July 2023.

**Abstract:** Urban heat islands, characterized by higher temperatures in cities compared to surrounding areas, have been studied using various techniques. However, during heat waves, existing models often underestimate the intensity of these heat islands compared to empirical measurements. To address this, an hourly time-series-based model for predicting heat island intensity during heat wave conditions is proposed. The model was developed and validated using empirical data from the National Monitoring Network in Temuco, Chile. Results indicate a strong correlation ( $r > 0.98$ ) between the model's predictions and actual monitoring data. Additionally, the study emphasizes the importance of considering the unique microclimatic characteristics and built environment of each city when modelling urban heat islands. Factors such as urban morphology, land cover, and anthropogenic heat emissions interact in complex ways, necessitating tailored modelling approaches for the accurate representation of heat island phenomena.

**Keywords:** urban heat islands; heat waves; prediction model



**Citation:** Martinez-Soto, A.; Fürle, J.; Zipf, A. Urban Heat Island Intensity Prediction in the Context of Heat Waves: An Evaluation of Model Performance. *Eng. Proc.* **2023**, *39*, 80. <https://doi.org/10.3390/engproc2023039080>

Academic Editors: Ignacio Rojas, Hector Pomares, Luis Javier Herrera, Fernando Rojas and Olga Valenzuela

Published: 12 July 2023



**Copyright:** © 2023 by the authors. Licensee MDPI, Basel, Switzerland. This article is an open access article distributed under the terms and conditions of the Creative Commons Attribution (CC BY) license (<https://creativecommons.org/licenses/by/4.0/>).

## 1. Introduction

An urban heat island (UHI) is defined as the temperature difference observed between urban areas and the surrounding rural regions [1]. UHIs can occur in any season of the year and any time of day [2]. However, their effects are more noticeable during periods of temperature increase (e.g., heatwaves in summer). The increase in global temperatures due to global warming intensifies the effect of urban heat islands [3]. As the ambient temperature rises, urban areas experience even higher temperatures [4].

High temperatures in heat islands lead to the need for air conditioning and cooling in buildings, which increases energy consumption and results in higher greenhouse gas emissions, further contributing to global warming [5,6]. Furthermore, high temperatures can have adverse health effects on individuals, such as heat strokes, dehydration, and respiratory problems. For example, during the summer of 2003 in Europe, more than 70,000 additional deaths were attributed to heat waves [7]. Elderly individuals and households without access to air conditioning systems are identified as the first at-risk group. However, this risk level increases in urban heat islands, making the identification of these areas crucial for the development of mitigation measures (e.g., incorporating green spaces or planning open spaces that promote air circulation and shade), as well as for the protection of people.

Various techniques are employed to map urban heat islands in cities [8–10]. These include satellite remote sensing for large-scale temperature assessment, ground-based sensors and weather stations for real-time and precise data collection, aerial thermography using infrared cameras mounted on aircraft or drones to obtain detailed thermal images,

on-site temperature measurements using portable thermometers or thermographic devices, and simulation models that incorporate urban geometry, land use, vegetation, and solar radiation to predict and map heat islands [11–19]. A combination of these techniques and data sources is crucial to gain a comprehensive understanding of heat islands, enabling informed decision-making in urban planning, mitigation strategies, and the informed safeguarding of residents' health [13,20].

This study presents a combined technique for locating heat islands in the city of Temuco, Chile, as a case study. Using data from 23 monitoring stations and utilizing QGIS, areas with higher temperatures were mapped. Subsequently, a methodology for predicting heat islands was proposed for days when the external temperature exceeded 30 degrees Celsius for 3 consecutive days (heatwaves). The results are validated by comparing modeled values for specific heat island sectors in the city with actual measurements taken during heatwave days in the summer of 2019. Due to the accuracy of the results ( $r > 0.98$ ), it is concluded that it is possible to predict the location of heat islands during heatwave events using the proposed methodology.

## 2. Methods

### 2.1. Case Study

Temuco is located in a valley surrounded by hills and mountains. The city sits at an altitude of approximately 350 m above sea level and is crossed by the Cautín River. The predominant vegetation in the area is the temperate rainforest, characteristic of the southern zone of Chile. Temuco is a relatively large city with a population of around 300,000 inhabitants. It is an urban center that is constantly growing and developing. The city is an important commercial, educational, and cultural hub in the region, offering a wide range of services and activities.

### 2.2. Measurement of the Temperature and Mapping of the Heat Island

To measure the temperature in different sectors of the city, monitoring stations belonging to the National Monitoring Network (ReNaM) of Chile were used. The network in Temuco consists of 23 weather stations (from Netatmo) represented by black dots in Figure 1, which are installed in private properties across various zones in Temuco.

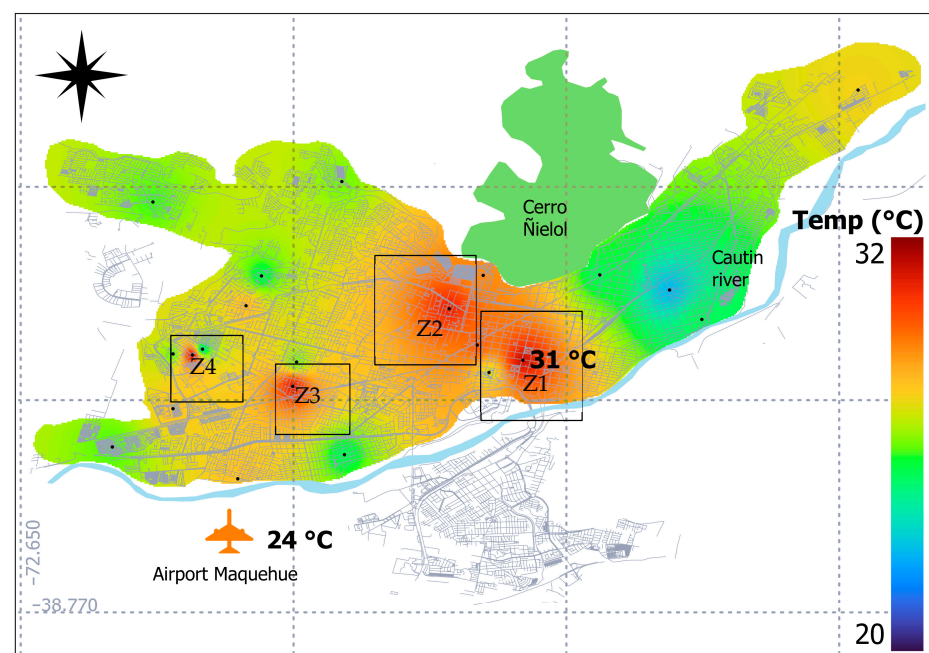


**Figure 1.** Mapping of the UHI phenomenon in Temuco using fixed station methodology (left) and IDW interpolation in QGIS. Temperatures from 4 December 2019, at 2 pm, are taken into account.

The Netatmo weather stations comprise two devices (indoor and outdoor) made of UV-resistant aluminum, capable of measuring temperatures ranging from  $-40\text{ }^{\circ}\text{C}$  to  $65\text{ }^{\circ}\text{C}$  with an accuracy of  $\pm 0.3\text{ }^{\circ}\text{C}$ . The outdoor sensors are shielded from rain and direct sunlight to prevent deterioration and to ensure better data accuracy. Data are captured at thirty-minute intervals, following a fixed schedule to maintain consistency (e.g., 8:00–8:30–9:00, etc.). The sensors underwent calibration and validation by the Ministry of Housing and Urban Development (MINVU) in collaboration with the Chile Foundation.

For the geolocation of heat islands, individual values from each station were used at the same hour (e.g., 2 pm). Subsequently, the temperature values along with the station coordinates were inputted into the QGIS software. The IDW interpolation technique was employed in QGIS to map the heat islands into a continuous space within the city (Figure 1). In Figure 1, the spatial distribution of temperatures measured in the city on 4 December 2019, at 2 pm, is shown. Here, there are four zones in the city (Z1–Z4) where the temperature is higher than the measurement taken in the outer part of the city (Maquehue Airport). In Z1 and Z2 the central part of the city (characterized by higher building density and low vegetation), it is observed that the temperature ( $31\text{ }^{\circ}\text{C}$ ) is  $7\text{ }^{\circ}\text{C}$  higher than at the Maquehue Airport station ( $24\text{ }^{\circ}\text{C}$ ).

### 2.3. Prediction of Heat Islands during Heatwaves

To predict the intensity of heat islands in the city of Temuco, temperature differences were observed/analyzed between the weather station at Maquehue Airport and the stations situated in the four zones within the city that recorded the highest temperatures. The study specifically focused on visualizing the characteristics of heat islands during two heatwave episodes (referred to as HW1 and HW2) that occurred during the summer of 2020. By recording the temperature differences, Equation (1) has been formulated to describe the temperature in the 4 zones in the city (with the highest temperatures Z1–Z4) as a function of the temperature at Maquehue ( $TR$  = reference temperature) for each hour. Subsequently, these equations have been used to generate a general 24 h model that predicts the temperature in the four sectors of the city based on the temperature recorded at the Maquehue Airport station.

$$T_{i,z}(TR_i) = a_{i,z}TR_i + b_{i,z} \quad (1)$$

where:

$T$  = temperature;

$TR$  = reference temperature (measured at the Maquehue airport);

$i$  = time of a day in hours (1, 2 . . . 24);

$z$  = zone in Temuco where heat islands are identified (1, 2, 3, 4).

## 3. Results

### 3.1. Measurement and Recording of Temperatures during Heatwave Conditions

In Figure 2, a temperature comparison appears for two heat wave episodes (HW1 and HW2) that occurred in February 2020 between the Maquehue station (blue and red line respectively) and the zones with the highest temperature in Temuco (Z-1 to Z-4 in Figure 1). Here, it is observed first that the maximum temperature in Temuco occurs between 3 pm and 5 pm, which represents a behavior that does not follow the common pattern of the UHI phenomenon. The maximum temperature peak in most of the cases studied was reached between 7 pm and 8 pm. However, in the case of Temuco at that time, the temperature in the city dropped, whereas outside the city (reference temperature in Maquehue airport) the temperature reached its daily maximum.

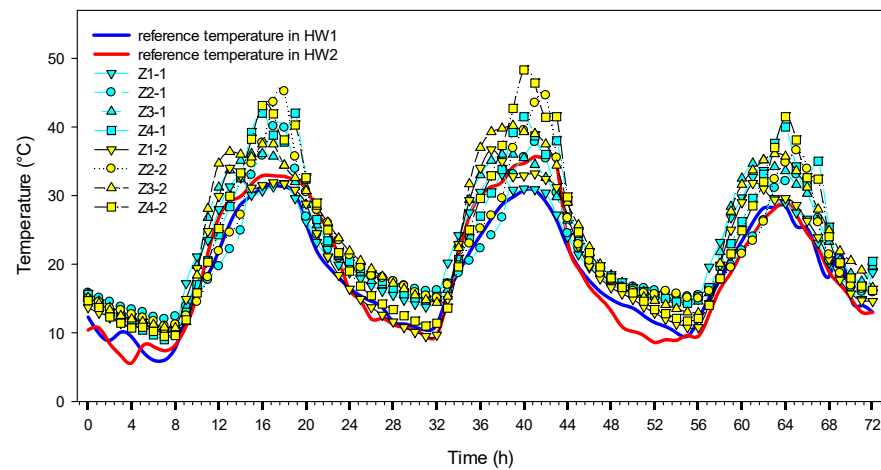


**Figure 2.** Comparison of temperature for two heat wave episodes between Maquehue station ((blue and red line respectively)) and the zones with the highest temperature in Temuco (Z1, Z2, Z3, Z4). Date for heat wave 1 (HW1): 8–10 February 2020. Date for heat wave 2 (HW2): 20–22 February 2020.

Additionally, the maximum temperatures recorded in the city had an average increase of 26 °C in a short period of time (between 10 am and 3 pm). The same speed of temperature change appeared from 4 pm where it reached on average 5.3 °C per hour. This is higher than the maximum acceptable temperature change rate (3 °C/h), which is set to prevent the human body from suddenly feeling hot or cold. This suggests the need to conduct more detailed studies on the behavior of the phenomenon in Temuco. Analyzing from the materiality of constructions, green areas, etc., several factors may explain more precisely the behavior of the UHI phenomenon in Temuco.

### 3.2. Prediction of Temperatures during Heatwave Conditions

Using Equation (1), the temperature profiles of the zones with the highest temperatures in the city (Z1, Z2, Z3, and Z4) have been predicted based on the temperature recorded at Maquehue (HW3) during a new heatwave that occurred on March 2020. The predicted temperatures were compared with the actually recorded temperatures during the third heatwave that took place between March 1st and March 3rd in order to validate the model and verify the accuracy of the results (Figure 3). Figure 3 shows a comparison between the temperature modeling for Zone 1 using temperatures from the reference station and the actual measured temperatures.

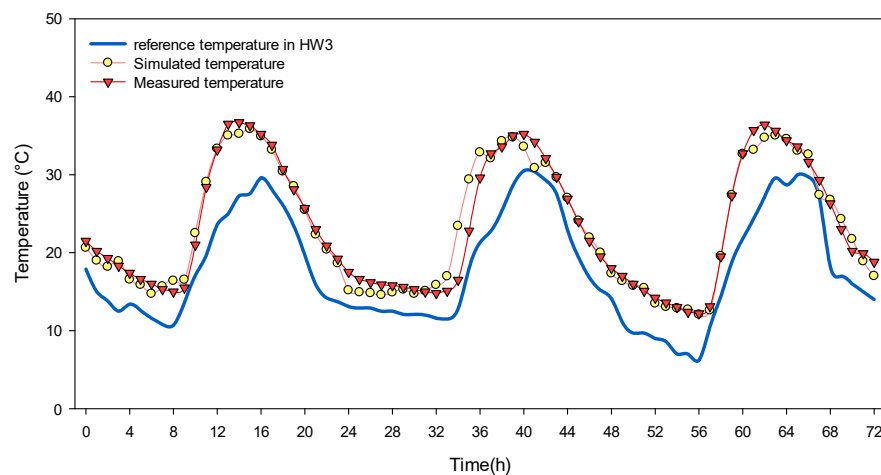


**Figure 3.** Comparison of real and modeled temperature profiles for zone 1 in Temuco based on the temperatures of the Maquehue station (HW3) located outside the city. Date: 1–3 March 2020.

Figure 3 shows that the values obtained from the modeling are very close to the real temperature profiles that occurred during that same heat wave event. Here, it was determined that the average real and modeled temperature differences in the 72-h period reached 1 °C and the correlation coefficient was 0.98. This strong correlation suggests it is possible to determine the temperature in the different zones of the city from the temperature of the weather station located outside the city (Maquehue). This would also imply that it is possible to know the past profiles and make a prediction for future heat wave events based on climate change scenarios. Nevertheless, additional studies are needed to verify these hypotheses and, in that sense, they represent a continuation of the work presented here.

In this study, different equations were developed to predict temperatures in each zone of the city and for each hour. Since each equation is specific to its respective zone and cannot be transferred to other zones, it follows that the modeling of heat islands cannot be generalized into a single predictive model for heat islands. Instead, each zone must be studied within its unique microclimate.

The study strongly emphasizes the critical importance of considering the distinct microclimatic characteristics and built environment of individual cities when modeling urban heat islands. The complex interplay among various factors, such as urban morphology, land cover properties, and anthropogenic heat emissions, requires the adoption of customized modeling approaches to accurately represent the phenomenon of heat islands.

By acknowledging these factors and employing tailored modeling techniques, a more precise representation of heat island phenomena can be achieved. This highlights the need for site-specific analyses and modeling in order to understand and mitigate the impact of heat islands in urban environments.

#### 4. Conclusions

The results of this study demonstrate the close alignment between the modeled and actual temperature profiles during the heatwave event, highlighting their significance in predicting heat islands. Notably, the average temperature differences between the real and modeled data over the 72 h period were only 1 °C, with a high correlation coefficient of 0.98. This strong correlation suggests the feasibility of estimating temperatures in various city zones based on measurements from the weather station located outside the city (Maquehue). The implications of accurate heat island predictions are substantial, as they directly impact public health and energy consumption. Furthermore, these findings open the possibility of retrospectively analyzing past temperature profiles and forecasting future heatwave events under different climate change scenarios. However, further studies are required to validate these hypotheses, representing a natural continuation of the research presented here.

**Author Contributions:** Conceptualization and methodology, A.M.-S.; software, A.M.-S.; formal analysis, A.M.-S. and J.F.; investigation, A.M.-S.; resources, A.M.-S.; writing—original draft preparation, A.M.-S. and J.F.; writing—review and editing, A.M.-S. and J.F.; supervision, A.Z.; funding acquisition, A.M.-S. All authors have read and agreed to the published version of the manuscript.

**Funding:** This research received no external funding.

**Institutional Review Board Statement:** Not applicable.

**Informed Consent Statement:** Not applicable.

**Data Availability Statement:** The data presented in this study are openly available in FigShare at <https://doi.org/10.6084/m9.figshare.20186816.v1>.

**Conflicts of Interest:** The authors declare no conflict of interest.



## References

1. García-Cueto, O.R.; Jáuregui-Ostos, E.; Toudert, D.; Tejeda-Martinez, A. Detection of the Urban Heat Island in Mexicali, BC, México and Its Relationship with Land Use. *Atmosfera* **2007**, *20*, 111–131.
2. Kuznetsova, I.N.; Brusova, N.E.; Nakhaev, M.I. Moscow Urban Heat Island: Detection, Boundaries, and Variability. *Russ. Meteorol. Hydrol.* **2017**, *42*, 305–313. [\[CrossRef\]](#)
3. Feinberg, A. Urban Heat Island Amplification Estimates on Global Warming Using an Albedo Model. *SN Appl. Sci.* **2020**, *2*, 2178. [\[CrossRef\]](#)
4. Liu, Z.; Zhan, W.; Bechtel, B.; Voogt, J.; Lai, J.; Chakraborty, T.; Wang, Z.H.; Li, M.; Huang, F.; Lee, X. Surface Warming in Global Cities Is Substantially More Rapid than in Rural Background Areas. *Commun. Earth Environ.* **2022**, *3*, 219. [\[CrossRef\]](#)
5. Narumi, D.; Levinson, R.; Shimoda, Y. Effect of Urban Heat Island and Global Warming Countermeasures on Heat Release and Carbon Dioxide Emissions from a Detached House. *Atmosphere* **2021**, *12*, 572. [\[CrossRef\]](#)
6. Santamouris, M.; Cartalis, C.; Synnefa, A.; Kolokotsa, D. On the Impact of Urban Heat Island and Global Warming on the Power Demand and Electricity Consumption of Buildings—A Review. *Energy Build.* **2015**, *98*, 119–124. [\[CrossRef\]](#)
7. Robine, J.M.; Cheung, S.L.K.; Le Roy, S.; Van Oyen, H.; Griffiths, C.; Michel, J.P.; Herrmann, F.R. Death Toll Exceeded 70,000 in Europe during the Summer of 2003. *Comptes Rendus-Biol.* **2008**, *331*, 171–178. [\[CrossRef\]](#) [\[PubMed\]](#)
8. Hashim, N.M.; Ahmad, A.; Abdullah, M. Mapping Urban Heat Island Phenomenon: Remote Sensing Approach. *J.-Inst. Eng.* **2007**, *68*, 25–30.
9. Elmarakby, E.; Khalifa, M.; Elshater, A.; Afifi, S. Tailored Methods for Mapping Urban Heat Islands in Greater Cairo Region. *Ain Shams Eng. J.* **2022**, *13*, 101545. [\[CrossRef\]](#)
10. Abrar, R.; Sarkar, S.K.; Nishtha, K.T.; Talukdar, S.; Shahfahad; Rahman, A.; Islam, A.R.M.T.; Mosavi, A. Assessing the Spatial Mapping of Heat Vulnerability under Urban Heat Island (UHI) Effect in the Dhaka Metropolitan Area. *Sustainability* **2022**, *14*, 4945. [\[CrossRef\]](#)
11. Kopecká, M.; Szatmári, D.; Holec, J.; Feranec, J. Urban Heat Island Modelling Based on MUKLIMO: Examples from Slovakia. *AGILE GIScience Ser.* **2021**, *2*, 5. [\[CrossRef\]](#)
12. Hafner, J.; Kidder, S.Q. Urban Heat Island Modeling in Conjunction with Satellite-Derived Surface/Soil Parameters. *J. Appl. Meteorol.* **1999**, *38*, 448–465. [\[CrossRef\]](#)
13. Voelkel, J.; Shandas, V. Towards Systematic Prediction of Urban Heat Islands: Grounding Measurements, Assessing Modeling Techniques. *Climate* **2017**, *5*, 41. [\[CrossRef\]](#)
14. Wang, K.; Aktas, Y.D.; Stocker, J.; Carruthers, D.; Hunt, J.; Malki-Epshtein, L. Urban Heat Island Modelling of a Tropical City: Case of Kuala Lumpur. *Geosci. Lett.* **2019**, *6*, 4. [\[CrossRef\]](#)
15. Dorigon, L.P.; Amorim, M.C.d.C.T. Spatial Modeling of an Urban Brazilian Heat Island in a Tropical Continental Climate. *Urban Clim.* **2019**, *28*, 100461. [\[CrossRef\]](#)
16. Xu, M.; Bruelisauer, M.; Berger, M. Development of a New Urban Heat Island Modeling Tool: Kent Vale Case Study. *Procedia Comput. Sci.* **2017**, *108*, 225–234. [\[CrossRef\]](#)
17. Kubilay, A.; Allegrini, J.; Strebel, D.; Zhao, Y.; Derome, D.; Carmeliet, J. Advancement in Urban Climate Modelling at Local Scale: Urban Heat Island Mitigation and Building Cooling Demand. *Atmosphere* **2020**, *11*, 1313. [\[CrossRef\]](#)
18. Garzón, J.; Molina, I.; Velasco, J.; Calabia, A. A Remote Sensing Approach for Surface Urban Heat Island Modeling in a Tropical Colombian City Using Regression Analysis and Machine Learning Algorithms. *Remote Sens.* **2021**, *13*, 4256. [\[CrossRef\]](#)
19. Khan, A.; Chatterjee, S.; Wang, Y. *Urban Heat Island Modeling for Tropical Climates*; Elsevier: Amsterdam, The Netherlands, 2020.
20. Kim, S.W.; Brown, R.D. Urban Heat Island (UHI) Intensity and Magnitude Estimations: A Systematic Literature Review. *Sci. Total Environ.* **2021**, *779*, 146389. [\[CrossRef\]](#) [\[PubMed\]](#)

**Disclaimer/Publisher’s Note:** The statements, opinions and data contained in all publications are solely those of the individual author(s) and contributor(s) and not of MDPI and/or the editor(s). MDPI and/or the editor(s) disclaim responsibility for any injury to people or property resulting from any ideas, methods, instructions or products referred to in the content.